H. Kellay
CPMOH, U. Bordeaux 1

Some experiments displaying singular behavior

Thinning, break up, coalescence, and line undulations

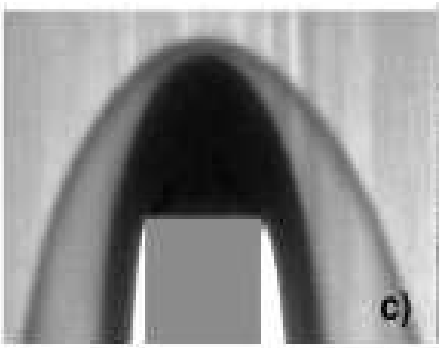

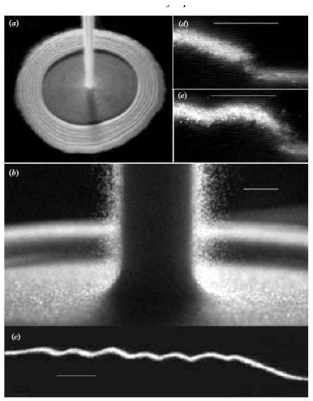

H. Kellay
Y. Amarouchene
J. F. Boudet
O. Greffier
G. Cristobal
N. François
F. Seychelles
M. Roche

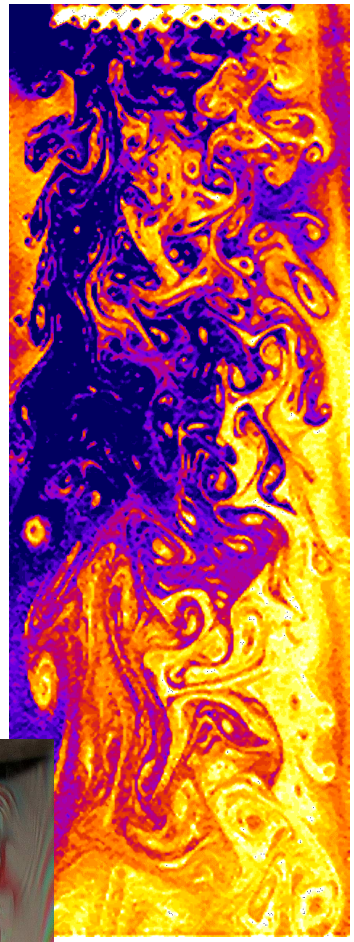

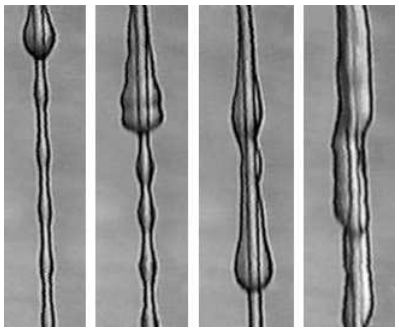

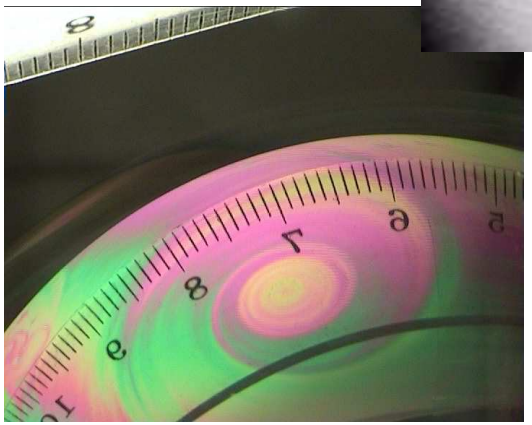

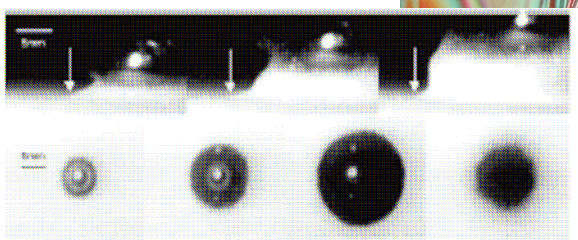

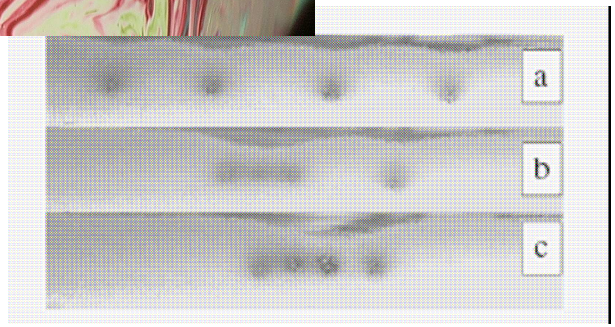

Saffman Taylor fingers

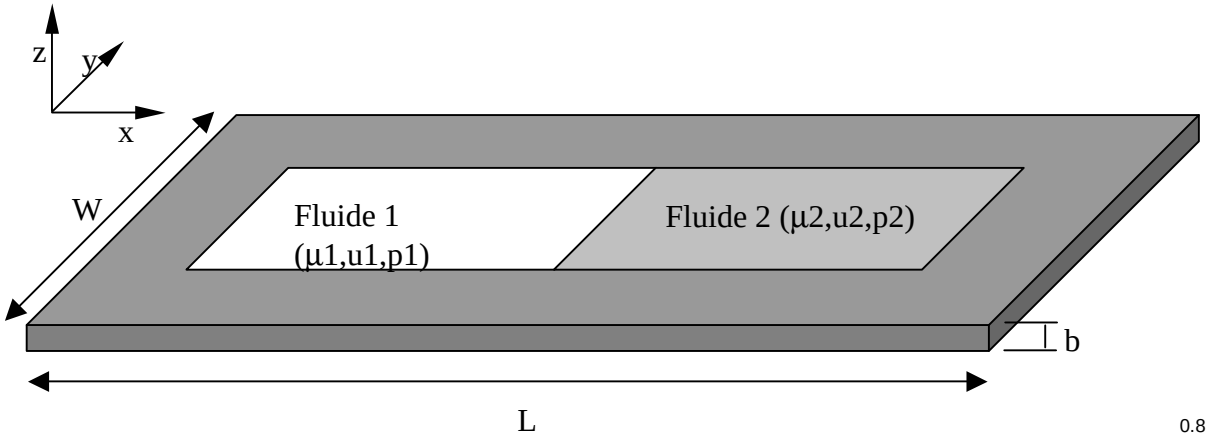

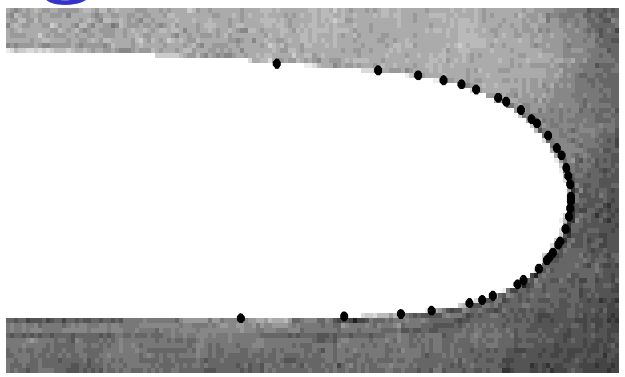

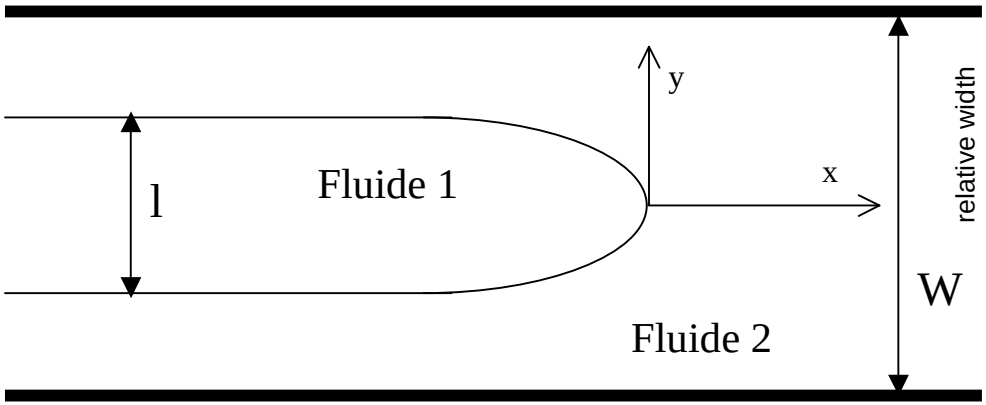

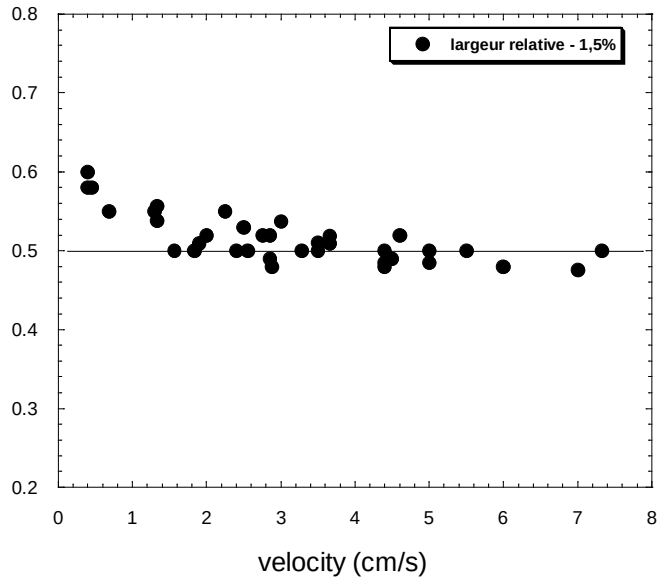

Finger thinning in a Hele Shaw cell

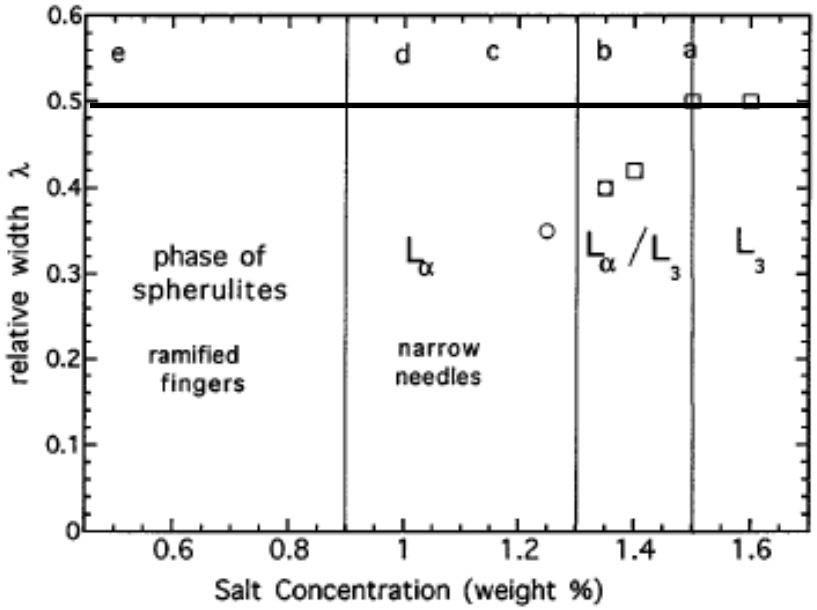

FIG. 1. Relative width as a function of salt concentration (circles: L_α phase; squares: L_3 phase) and phase boundaries of the surfactant-water-salt mixture at 7 wt % of surfactant. The letters *a* through *e* correspond to the photographs in Fig. 2.

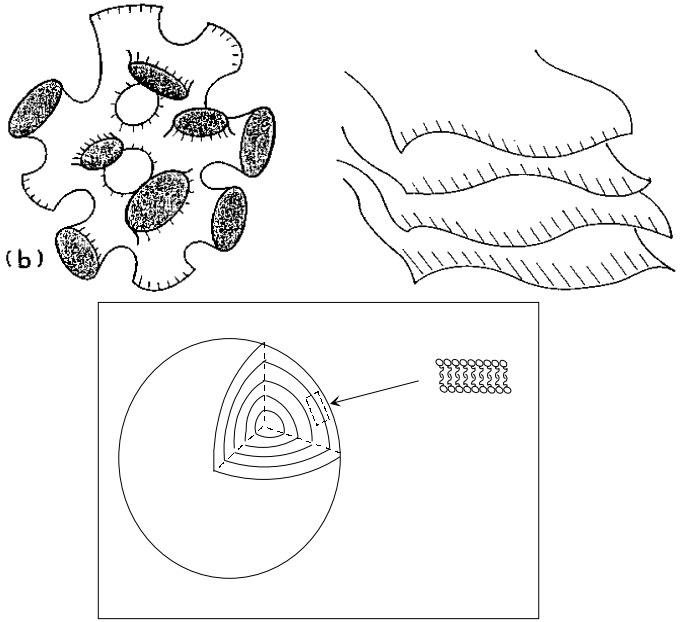

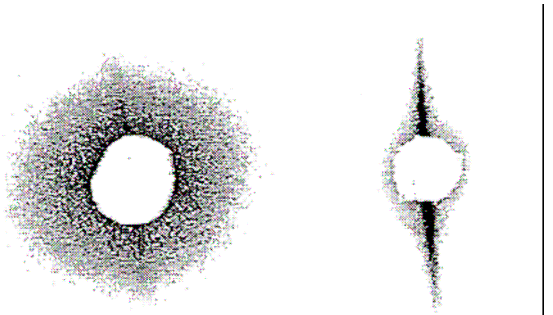

-'Observation of a finite time singularity in needle propagation in Hele-Shaw cells'
O. Greffier, A. Al Kahwaji, J. Rouch, and H. Kellay, Phys. Rev. Letts. 81, 3860, 1998.

Different phases different fingers

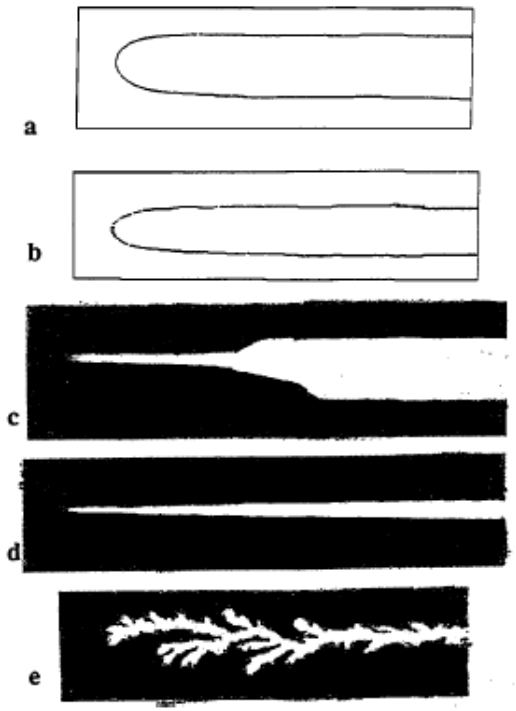

FIG. 2. Photographs of Fingers: (a) L_3 phase at 1.5% salt; (b) L_α phase at 1.35% salt; (c) L_α at 1.15% salt; (d) L_α at 1% salt; (e) spherulite phase at 0.5% salt.

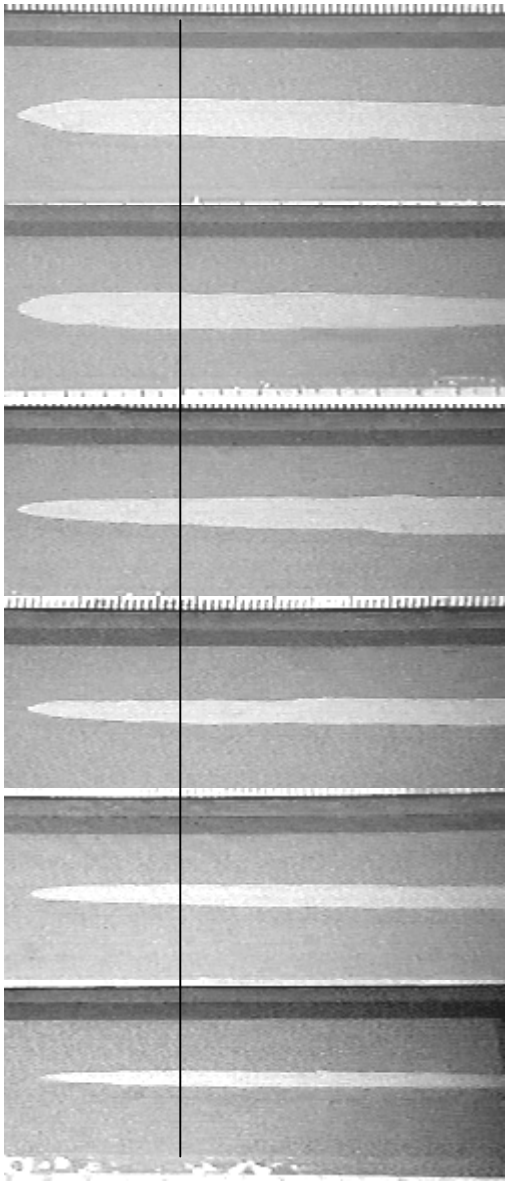

Finger thinning:

$$\lambda=\lambda_0(1-t/t_\lambda)^a$$

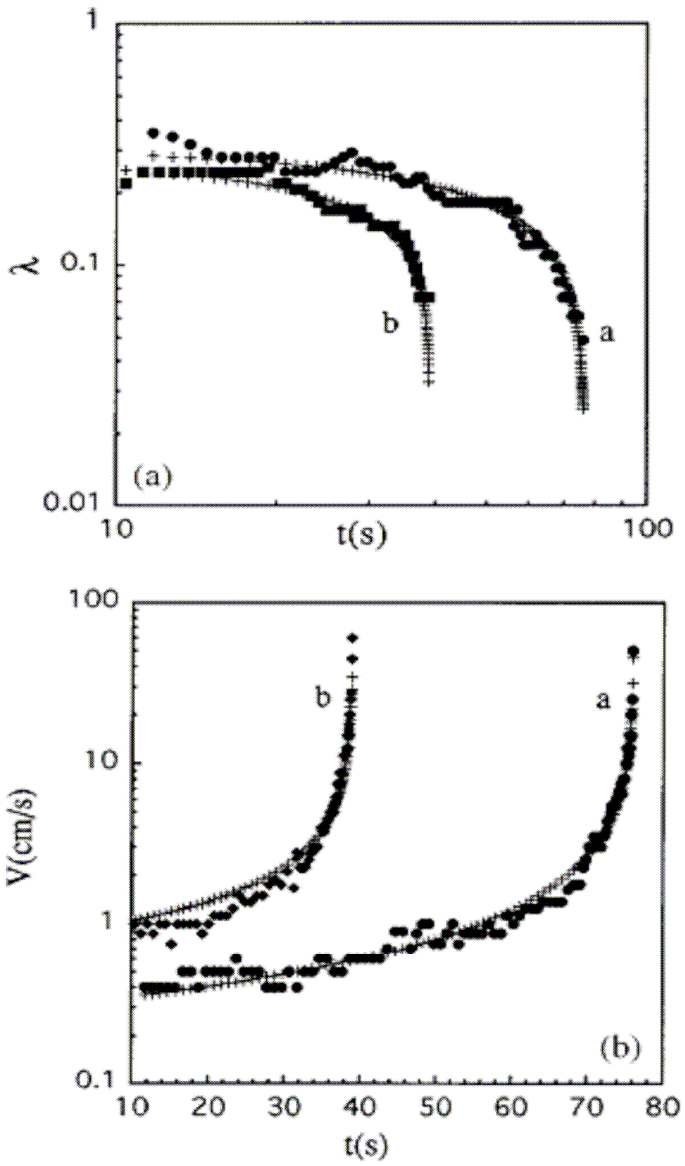

$$\frac{|\Delta P|}{L-x}=\frac{12\mu}{b^2}\lambda_0\left(1-\frac{t}{t_\lambda}\right)^a\frac{\partial x}{\partial t}$$

$$v(t)=\frac{L}{2t_c}\frac{1}{\left(1-\frac{t}{t_\lambda}\right)^a}\frac{1}{\sqrt{1-\frac{1}{1-a}\frac{t_\lambda}{t_c}+\frac{1}{1-a}\frac{t_\lambda}{t_c}\left(1-\frac{t}{t_\lambda}\right)^{1-a}}}$$

$$t_c=\frac{6\mu\lambda_0 L^2}{b^2|\Delta P|}$$

$$t_\lambda=(1-a)t_c$$

$$v(t)=\frac{L}{2t_c}\left(1-\frac{t}{t_\lambda}\right)^{-\frac{1+a}{2}}$$

Inhibition of a finite time singularity

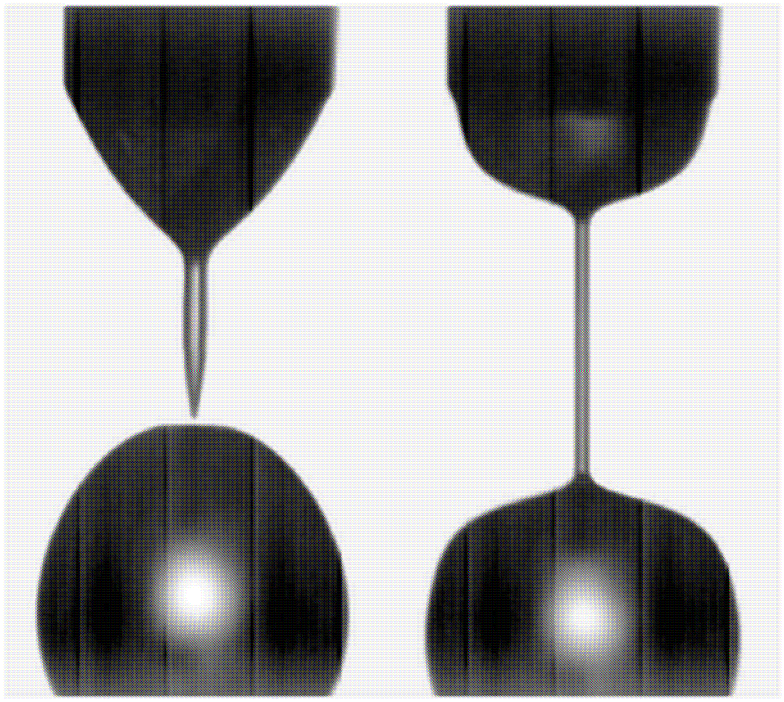

FIG. 1. Detachment of a pure water drop (left) and the detachment of a 100 ppm PEO (4×10^6 amu) polymer solution drop (right); note the formation of a long-lived filament.

'Inhibition of a finite time singularity in the droplet fission of a polymeric liquid'
Y. Amarouchene, D. Bonn, J. Meunier and H. Kellay. Phys. Rev Lett. 86, 3558 (2001)

Dynamics of thinning

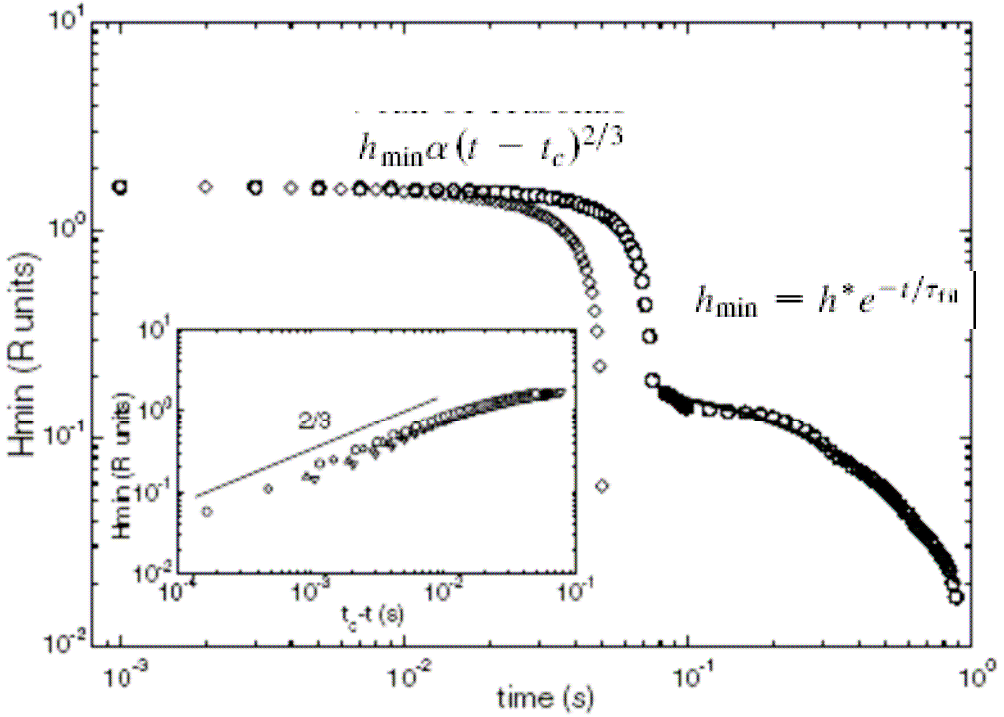

FIG. 2. Minimum neck thickness h_{min} for a pure water drop (diamonds) and for a 250 ppm PEO (4×10^6 amu) polymer solution drop (circles) along with an exponential fit for the second part of the curve. Note the kink in the second curve; this corresponds to the onset of filamentation as discussed in the text. The inset to the figure shows the neck thinning behavior for water (circles) and polymer solutions with 50 ppm (diamonds), 250 ppm (up triangles), and 750 ppm (down triangles). The polymer molecular weight here is 4×10^6. h_{min} has been rescaled by the capillary radius ($R = 2$ mm).

Why?

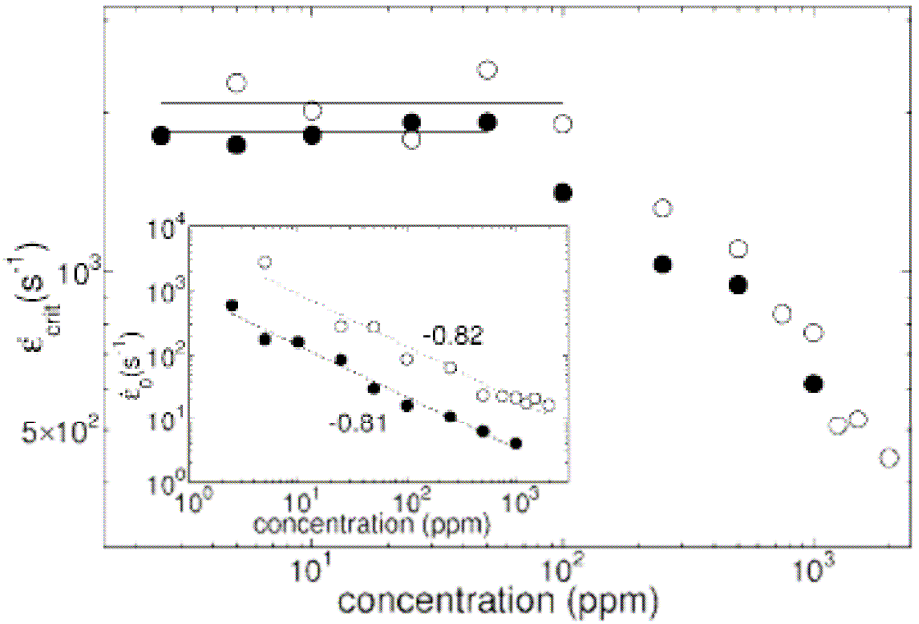

FIG. 3. The critical elongation rate for the onset of filament formation and the elongation rate for the filaments (inset) as a function of polymer concentration for the 8×10^6 (filled symbols) and the 4×10^6 (open symbols) molecular weights.

$$\varepsilon = dV_z/dz$$

$$\varepsilon = -2V_R/h_{min}$$

constant for filament

Rheological consequences

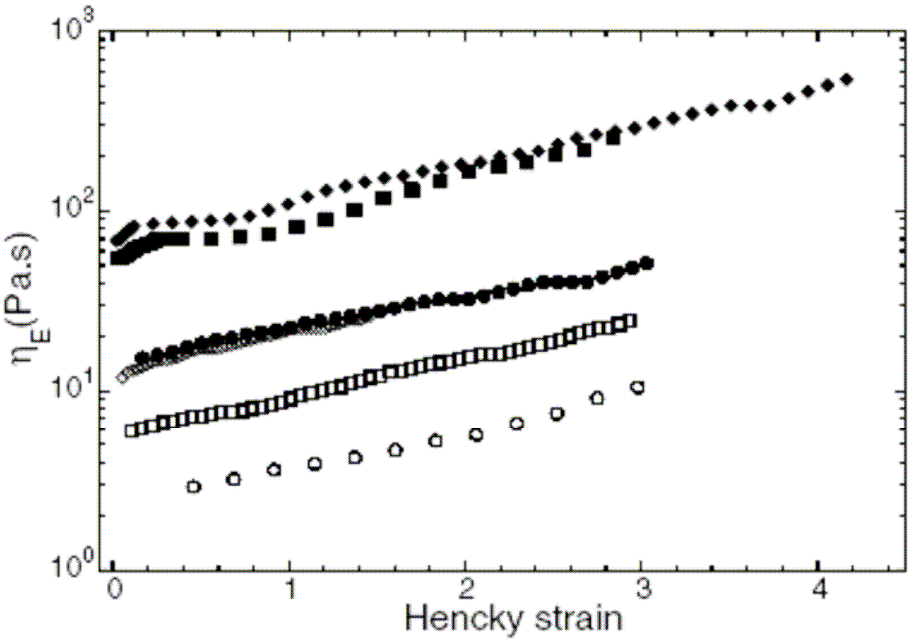

FIG. 4. Estimates of the elongational viscosity of the polymer solutions used versus the Hencky strain for the 8×10^6 (filled symbols) and the 4×10^6 (open symbols) molecular weights; 25 ppm (circles), 100 ppm (squares), and 250 ppm (diamonds).

Balance between cappilary stresses and elongational stresses:

$\eta_E \varepsilon_0 = 2\gamma / h_{min}$

Coalescence

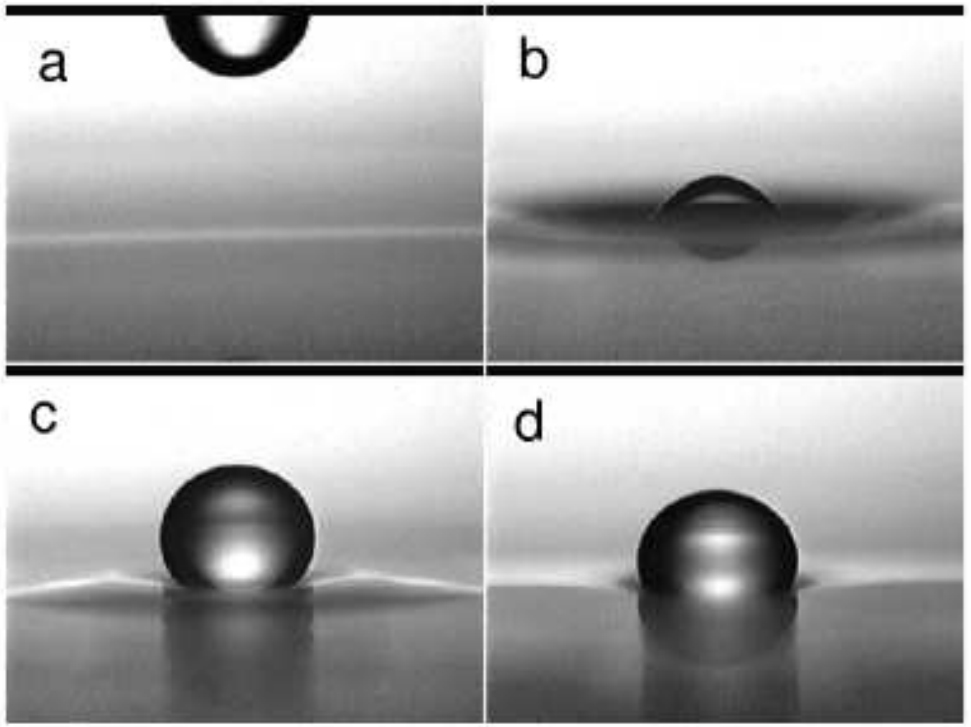

FIG. 1. Photograph of a drop of surfactant falling (a), impacting the surface (b), and rebounding (c) before coming to rest (d).

'Noncoalescencing drops' Y. Amarouchene, G. Cristobal, and H. Kellay, Phys. Rev. Letters, 87, 206104, (2001)

coalescence times and energy barrier

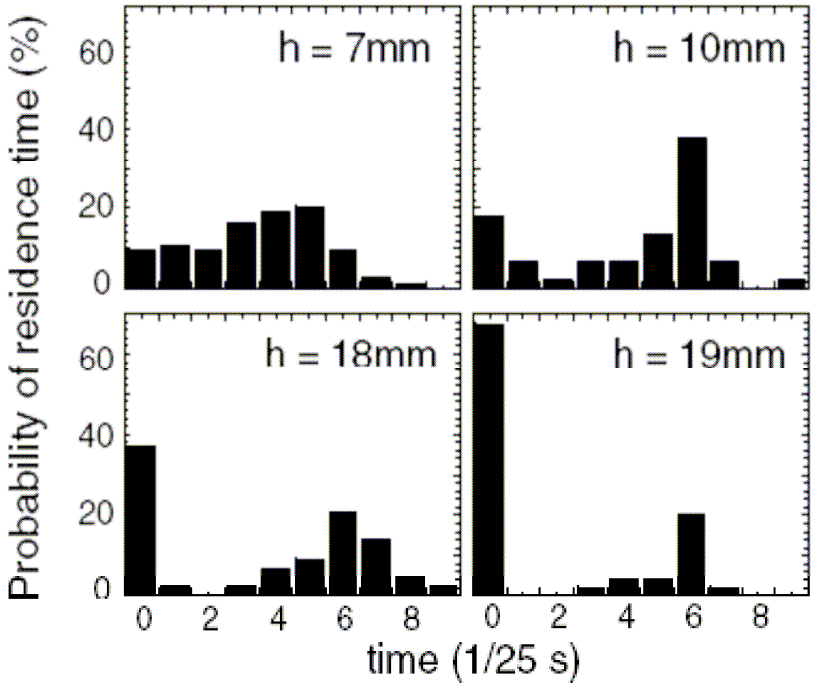

FIG. 2. Probability distributions of the residence time of a drop on the surface of the liquid for four different heights of release and 1 mM AOT solution.

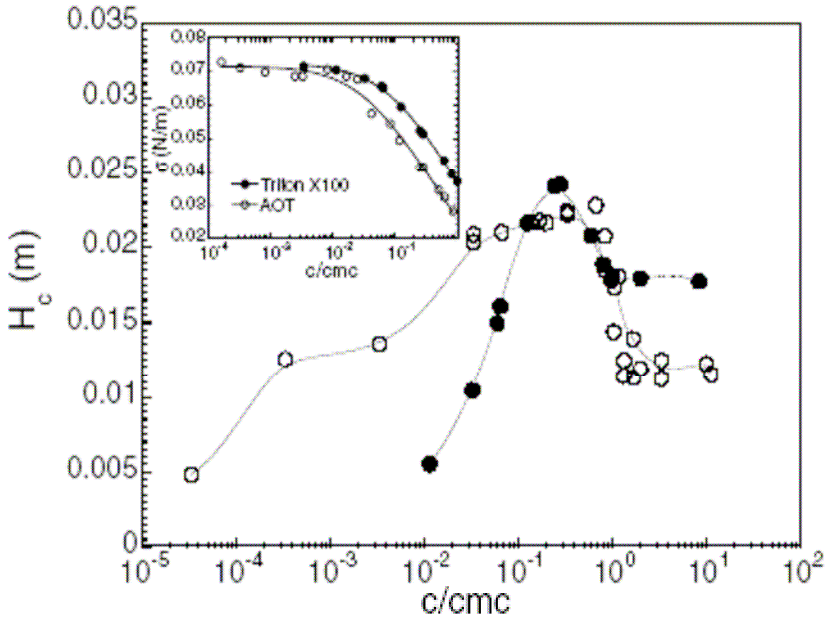

FIG. 3. The critical release height for coalescence to occur versus surfactant concentration and two different surfactant systems. Inset: Variation of surface tension versus concentration; the solid lines are fits using the Langmuir-Szyszkowski adsorption isotherm.

energy or energy per unit surface?

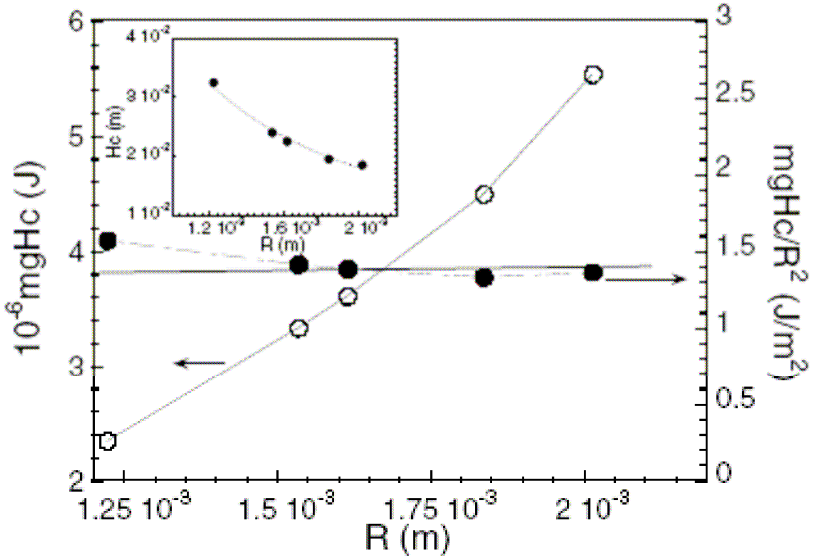

FIG. 4. Energy barrier and energy barrier normalized by the square of the drop radius R versus R for a concentration of 1 mM AOT. Inset: Variation of h_c versus R.

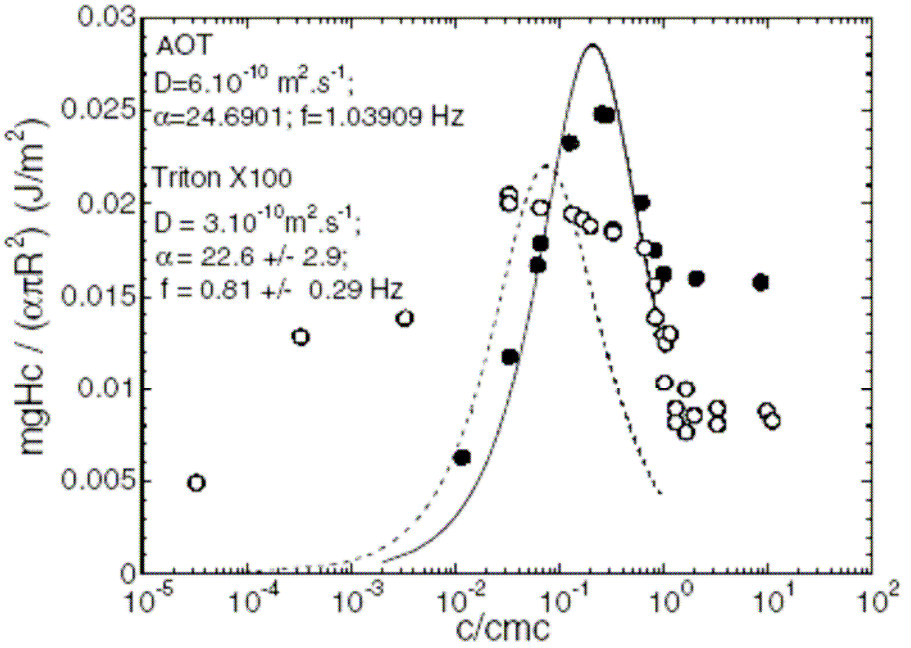

FIG. 5. The energy barrier per unit surface versus concentration for the two surfactant systems. The solid lines are fits using the Lucassen model.

what sets the critical time?

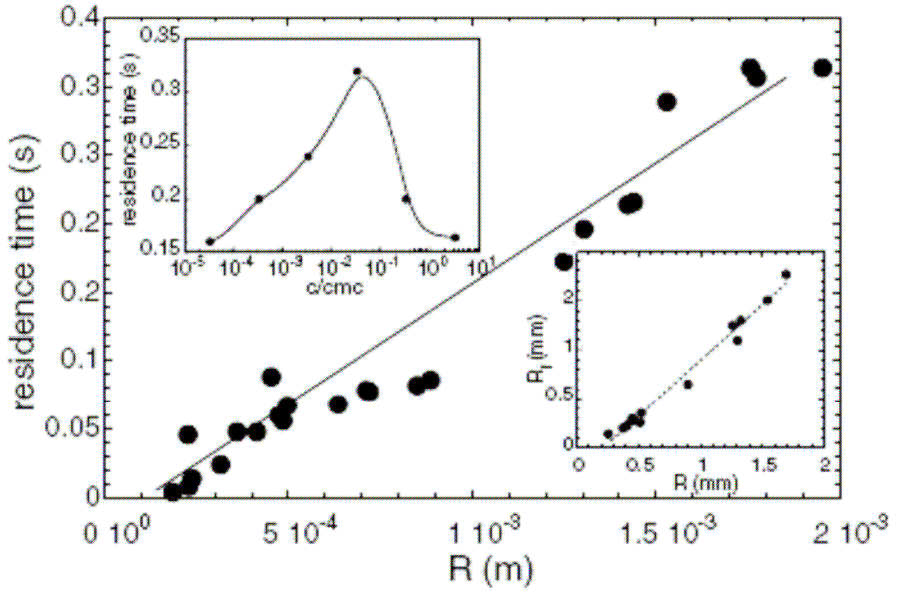

FIG. 6. Residence time versus drop radius for a fixed surfactant concentration (10 mM AOT). Upper inset: Variation of the residence time versus concentration (AOT system). Lower inset: Radius R_f of the contact area (A) between drop and surface versus R.

Reynolds draining

$t_c=(A^2\mu/F)(d_c^{-2}-d_i^{-2})$

A contact area

F=mg

d_c ~ 1micrometer

Conformation statistics of a deformable line

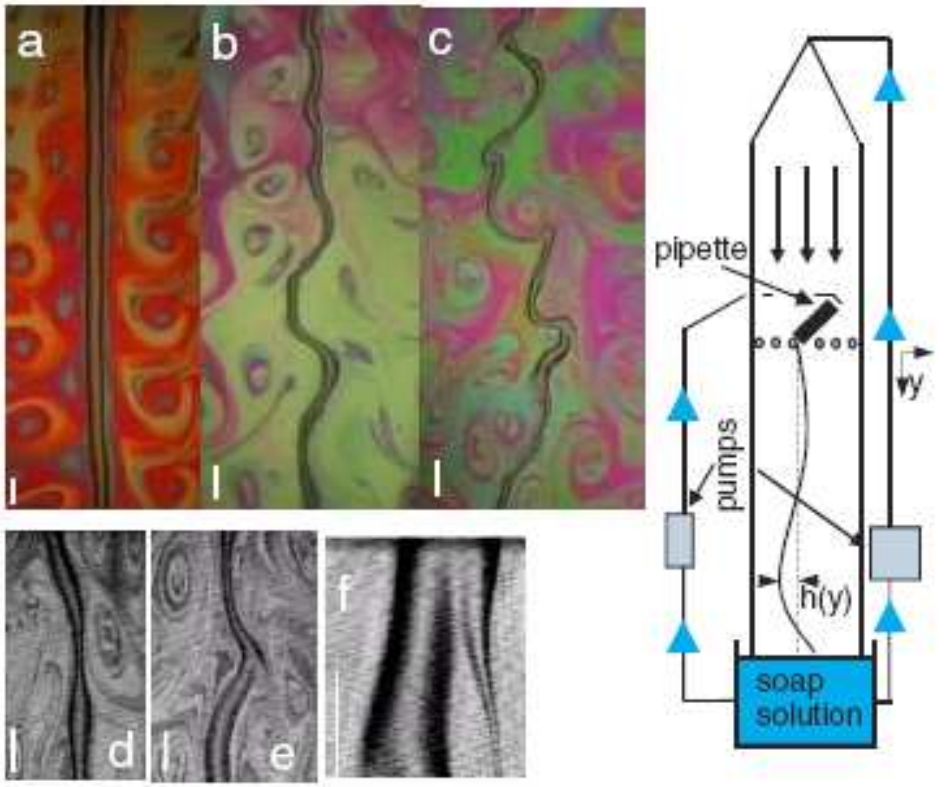

FIG. 1 (color online). Schematic of the experimental setup where the wiggly line in the middle of the channel represents the liquid column. Photographs of the column at increasing turbulence intensities from left to right [(a)–(c) for which the turbulent intensity is 5%, 9%, and 14%, respectively, for a column flux of 0.12 ml/s (a) and 0.06 ml/s, (b) and (c)]. Photographs of the column thickness modulations (for a turbulent intensity of 14%) (d) and singularities (turbulent intensity of 15%) (e). (f) A zoom on the singularity seen in (e). The white bars represent a distance of 2 mm except for figure (f) where the bar is 1 mm in length.

'Conformation Statistics of a Deformable Material Line in Two Dimensional Turbulence'
Y. Amarouchene and H. Kellay,
Physical Review Letters, 95, 054501, (2005) .

waves on a liquid string?

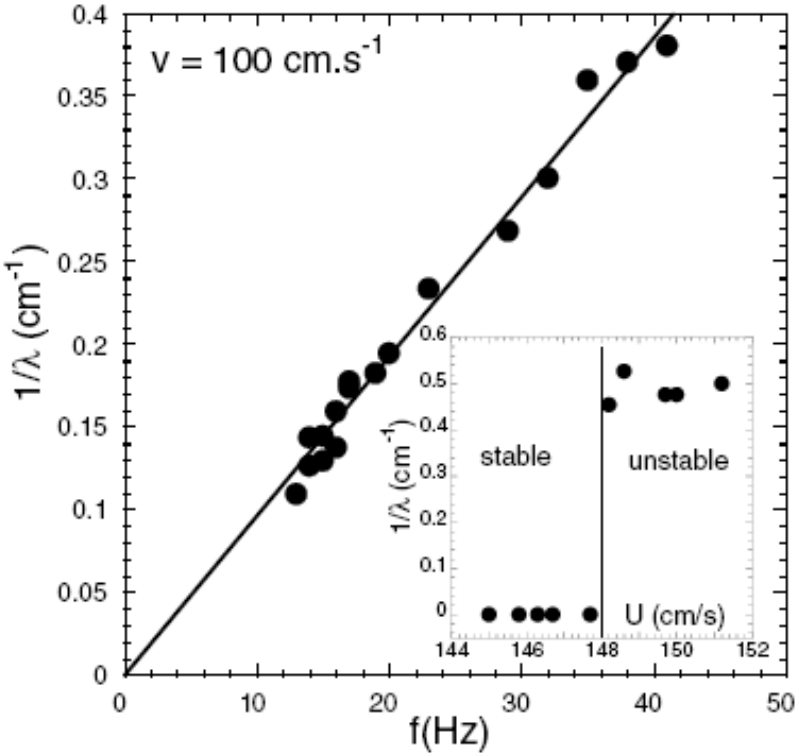

FIG. 2. Dispersion relation: Inverse wave number versus the driving frequency, in the laminar film (the flux of the film is 0.2 ml/s and the flux of the column is 0.1 ml/s). Inset: Most unstable wavelength in the laminar film; note the sharp transition near a velocity of 148 cm/s; the column flux is 0.06 ml/s.

$$\partial^2 h/\partial t^2 = \frac{T/\rho \partial^2 h/\partial y^2}{[1 + (\partial h/\partial y)^2]^{3/2}} + F(v)/\rho, \qquad (1)$$

and which can be approximated as

$$\partial^2 h/\partial t^2 = T/\rho \partial^2 h/\partial y^2 [1 - 3/2(\partial h/\partial y)^2] + F(v)/\rho. \qquad (2)$$

Structure functions

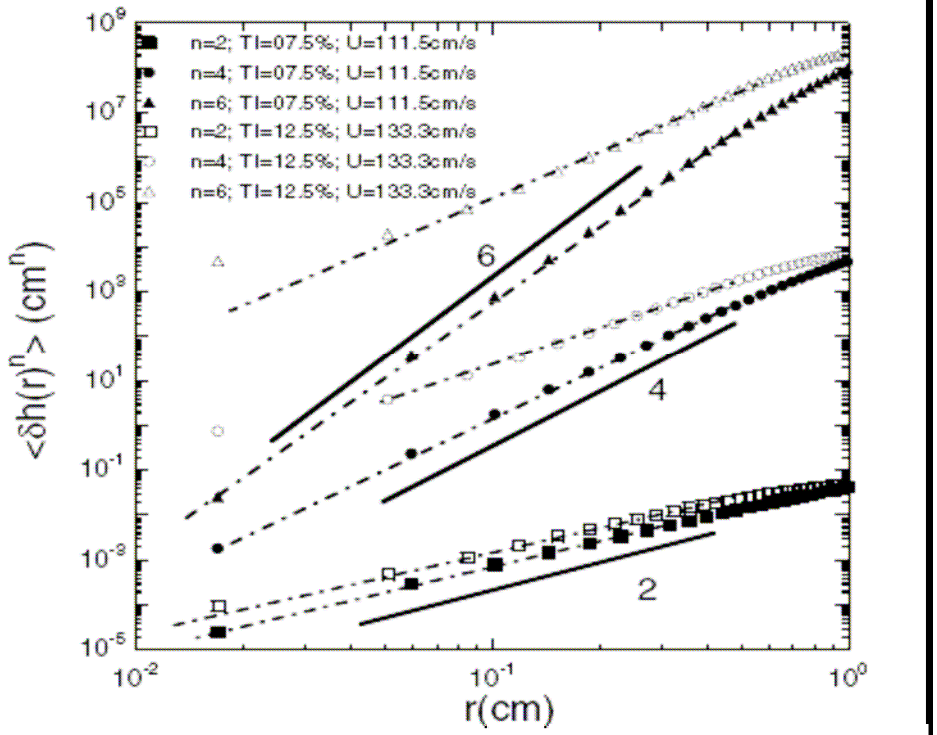

FIG. 3. Second, fourth, and sixth order structure functions for two different turbulent intensities. The straight line indicates the behavior for an analytic function. These moments were obtained by analyzing 1000 images giving over 510^5 data points. The turbulent intensities have an error of $\pm 0.1\%$.

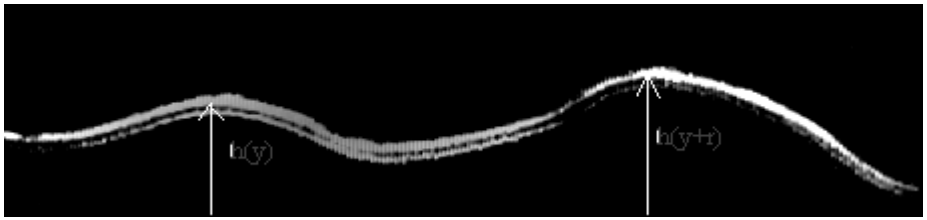

Intermittency? non analytic behavior?

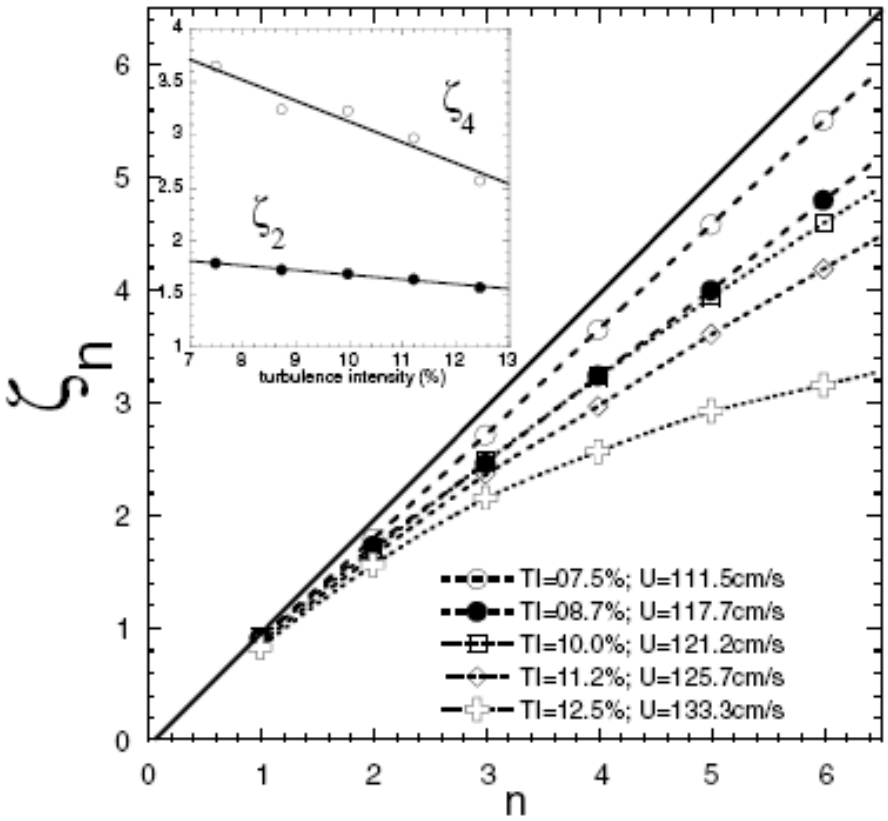

FIG. 4. Exponent ζ_n versus n for different turbulent intensities. Inset: ζ_2 and ζ_4 versus the turbulent intensity.

Conclusion

- Singularities arise often and sometimes come when they are not invited
- They can be inhibited
- They may be used to probe fluid properties
- They may help!